

Catalysis Under Alternating Magnetic Field: Rethinking the Origin of Enhanced Hydrogen Evolution Activities

Sitong Liu, Yudi Zhang, Wen Sun, Dandan Ma, Jinfu Ma, Zhiyang Wei, Juntao Huo,*
Dengsong Zhang,* and Guowei Li*

Magnetic fields are proposed to be a clean and powerful tool to boost the heterogeneous reaction processes, from the simple two-electron transfer hydrogen evolution to the complicated proton-coupling of multi-electron transfer reactions. Although many mechanisms are proposed to explain the field-assistant enhancement of activities, it remains an open question of how to understand the contradictory experiment results. In this study, the interplay between the alternating magnetic field (AMF) and the working electrodes from the viewpoint of their relative geometric positions is investigated. It is found that the HER current is almost doubled at an AMF of 25 mT when Pt foil and AMF are parallelly arranged, which is more significant than the perpendicularly arranged configuration. A significant increase in solution resistance is observed, which is in contradiction to previous works. The changing of currents with the AMF strength is investigated for the diamagnetic Cu, ferromagnetic Ni, and paramagnetic Ti and Pt wire, all suggesting the vital role of the induced electromotive force, which is a result of the relative geometric positions between the electrode and AMF. The findings provide an alternative mechanism for the magnetic field-assisted electrocatalytic processes, which is helpful for the rational design of high-performance catalysts.

fuel cell reaction.^[4,5] In the past few decades, great efforts have been devoted to increasing the catalytic activities, either by simply increasing the specific surface areas and the number of active sites,^[6,7] or boosting the intrinsic activities through strategies including doping,^[8,9] defect engineering,^[10] alloying, or introducing topological effect.^[11,12] However, the catalytic performance of emerging non-noble metal catalysts still cannot surpass that of traditional noble metal catalysts such as Pt. Thus, an ongoing challenge is to further enhance the catalytic activities in an economic and facile way.

Recently, external fields have become an emerging technique to regulate the structure of the catalyst and then tailoring the catalytic performance,^[13] including electric fields,^[14–16] strain, light,^[17–20] magnetic fields,^[21–23] or even gravitational fields.^[24,25] For example, the electric field can improve both conductivity and electron transmission of the catalysts, which will reduce the voltage


loss and then improve the HER performance.^[26] Most interestingly, the Gibbs free energy for hydrogen adsorption (ΔG_{H}) can also be optimized in the presence of the electric field.^[27] For oxygen evolution and reduction catalysts, the introduction of strain

1. Introduction

The development of efficient and durable catalysts is essential for the building of a sustainable energy future with heterogeneous processes such as water splitting,^[1,2] CO₂ reduction,^[3] and

S. Liu, Y. Zhang, W. Sun, Z. Wei, J. Huo, G. Li
CAS Key Laboratory of Magnetic Materials and Devices
Zhejiang Province Key Laboratory of Magnetic Materials and Application Technology
Ningbo Institute of Materials Technology and Engineering
Chinese Academy of Sciences
Ningbo 315201, China
E-mail: huojuntao@nimte.ac.cn; liguowei@nimte.ac.cn

S. Liu, D. Zhang
State Key Laboratory of Advanced Special Steel
School of Materials Science and Engineering
International Joint Laboratory of Catalytic Chemistry
College of Sciences
Shanghai University
Shanghai 200444, China
E-mail: dszhang@shu.edu.cn
Y. Zhang, W. Sun, Z. Wei, J. Huo
University of Chinese Academy of Sciences
19 A Yuquan Rd, Shijingshan District, Beijing 100049, China
D. Ma, J. Ma
School of Materials Science and Engineering
North Minzu University
Yinchuan 750021, China

 The ORCID identification number(s) for the author(s) of this article can be found under <https://doi.org/10.1002/apxr.202300067>

© 2023 The Authors. Advanced Physics Research published by Wiley-VCH GmbH. This is an open access article under the terms of the Creative Commons Attribution License, which permits use, distribution and reproduction in any medium, provided the original work is properly cited.

DOI: 10.1002/apxr.202300067

could change the energy band structure of the catalyst and thus improve intrinsic activities.^[28] For example, the catalyst on the right side of the peak of the volcanic map can reduce the overlap degree of *d*-orbital under the action of tensile stress. This will significantly lift the center of the *d*-orbital energy level and increase the density of states at the Fermi level. On the other hand, the catalyst on the left side of the volcanic peak assists can be optimized if a compressive strain is applied.^[29]

As a clean, low cost and non-intrusive method, magnetic fields have attracted more research attention in the optimization of catalytic activities.^[30–32] With a moderate magnetic field, water-splitting kinetics can be significantly promoted by using a ferromagnetic electrode such as Ni, Co, and their alloys.^[33–35] More interestingly, the reinforcement of catalytic efficiencies is strongly magnetism-independent, with the sequence for a better electrode as ferromagnetism (nickel), paramagnetism (platinum), and then nearly no effects on diamagnetism (graphite).^[36] Recent works highlight the important role of strongly correlated electrons during catalysis reactions because they are strongly connected with the *d*-orbital electron configuration and magnetic structures.^[37–39] Galán-Mascarós et al. studied the oxygen evolution reaction (OER) efficiencies of metal oxides with spinel structures and found strong magnetization-dependent activities.^[40] By carefully analyzing the relationship between the enhanced magneto-currents and magnetic moments of the spinel oxides, they proposed the vital role of the radical pair effect during the OER process. Albeit many studies have reported the vital role of spin polarization, the underlying mechanism for the interaction between OER intermediates, spin polarization, and magnetic fields remains unclear and keeping attracted fast-growing research interests.^[41–43] In a recent study, we used high-quality bulk single crystals to explore the influence of magnetic fields.^[44] Although the magnetization of the investigated Heusler alloys is much bigger than the previously reported metal oxides,^[45] we did not see any sign of OER activity enforcement. On the other hand, we found that the HER intrinsic catalytic activities can be suppressed significantly, for example, the turnover frequency of topological semimetal Co₂MnGa is decreased by 33%.^[46] In addition, the magnetism-independent reinforcement of catalytic efficiency can be explained by the magnetohydrodynamics effect induced by the Lorentz force, which acts either on ionic currents or oxygen/hydrogen bubble formation and release.^[47,48] Thus, how the magnetic fields “talk” with the chemical reactions requires more insightful exploration.

In this work, we observed a significant increase in HER activities for the Pt foil in the presence of AMF. To reveal the magnetic field-assisted mechanism, we investigated the influence of AMF on different metals including diamagnetic Cu, ferromagnetic Ni, and paramagnetic Ti and Pt wires. At a given potential, the current decreases to zero with the increase of AMF strength, suggesting the existence of an induced electromotive force that has an inverse sign with the applied potential. The contribution of temperature increase during the measurement is also ruled out by monitoring the temperature changes. Our findings suggest that the relative geometric position of the electrode in the magnetic field should be taken into consideration in the understanding of magneto-catalysis and can be used for the design of high-performance catalysis reactions.

2. Results and Discussion

2.1. Mechanisms for the Magneto Catalysis

Before the discussion of experimental details, let's first summarize the possible mechanisms for the enhanced catalytic activities in the presence of magnetic fields (Figure 1). One of the most accepted explanations is the magnetocaloric effect, which could speed the catalytic reactions by increasing the temperature (Figure 1a). In the presence of an external alternating magnetic field, the local temperature of the conducting catalysts is increased because of the existence of an eddy current or phase transition.^[49–50] This will certainly boost the activities according to the Arrhenius law.^[51] Another reason that comes easily to mind is the magnetoresistance effect.^[52] This will influence the resistivity and electron-hole separation properties of the catalysts, thus changing the electron transport behaviors during the electrocatalysis process (Figure 1b).^[53] If polarization happens, then Maxwell stress caused by the interaction between the magnetic field and dipole moment should be taken into consideration (Figure 1c).^[54] The generated Maxwell stress can change the shape of the paramagnetic droplets, which will affect the mass migration in the outer Helmholtz planes^[55] and thus improving the efficiency of electrocatalytic reactions. Similarly, the magnetohydrodynamic effect as a result of the Lorentz force will influence the motion of electrons and bubbles. Therefore, the desorption of bubbles on the surface of the catalyst can be accelerated, and the mass transfer effect can be improved (Figure 1d).^[56] The spin selectivity effects receive increasing research attention (Figure 1e). Both the reaction selectivity and efficiencies can be changed as a result of the radical pair effects.^[57–60]

2.2. HER under Alternating Magnetic Fields

In the first step, Pt foil is used to investigate the role of magnetic fields as it is one of the most promising HER catalysts. The measurements were carried out by using a standard three-electrode system, with Ag/AgCl and graphite rod as the reference and counter electrode, respectively (Figure S1, Supporting Information). The electrocatalysis cell filled with 1 M KOH is placed in vertical alternating magnetic fields up to 25 mT (Figure 2a). The photo of the experimental setup is shown in Figure S3 (Supporting Information). It can be seen clearly from the LSV curves that the HER activities of Pt foil are enhanced significantly in the presence of an AMF (Figure 2b). At the current density of 300 mA cm⁻² without a magnetic field, it requires an overpotential of 360 mV, which is in good agreement with previous studies. However, the overpotential is decreased to 348 mV with a small AMF of 5 mT, and then rapidly dropped to only 267 mV at 25 mT. To further highlight the enhanced activities, the field-dependent current density at an overpotential of 250 mV is displayed in Figure 2c. The current density increases from 120 mA cm⁻² without AMF to 250 mA cm⁻² at an AMF of 25 mT. We also recorded the current and voltage curves of Pt foil using chronopotentiometry (CP) and chronoamperometry (CA) methods (Figure S2, Supporting Information). In the presence of the AMF, the HER currents are increased and then return to their original value once the AMF is removed. Finally, the influence of AMF under acidic conditions (Figure S3, Supporting Information). Although the

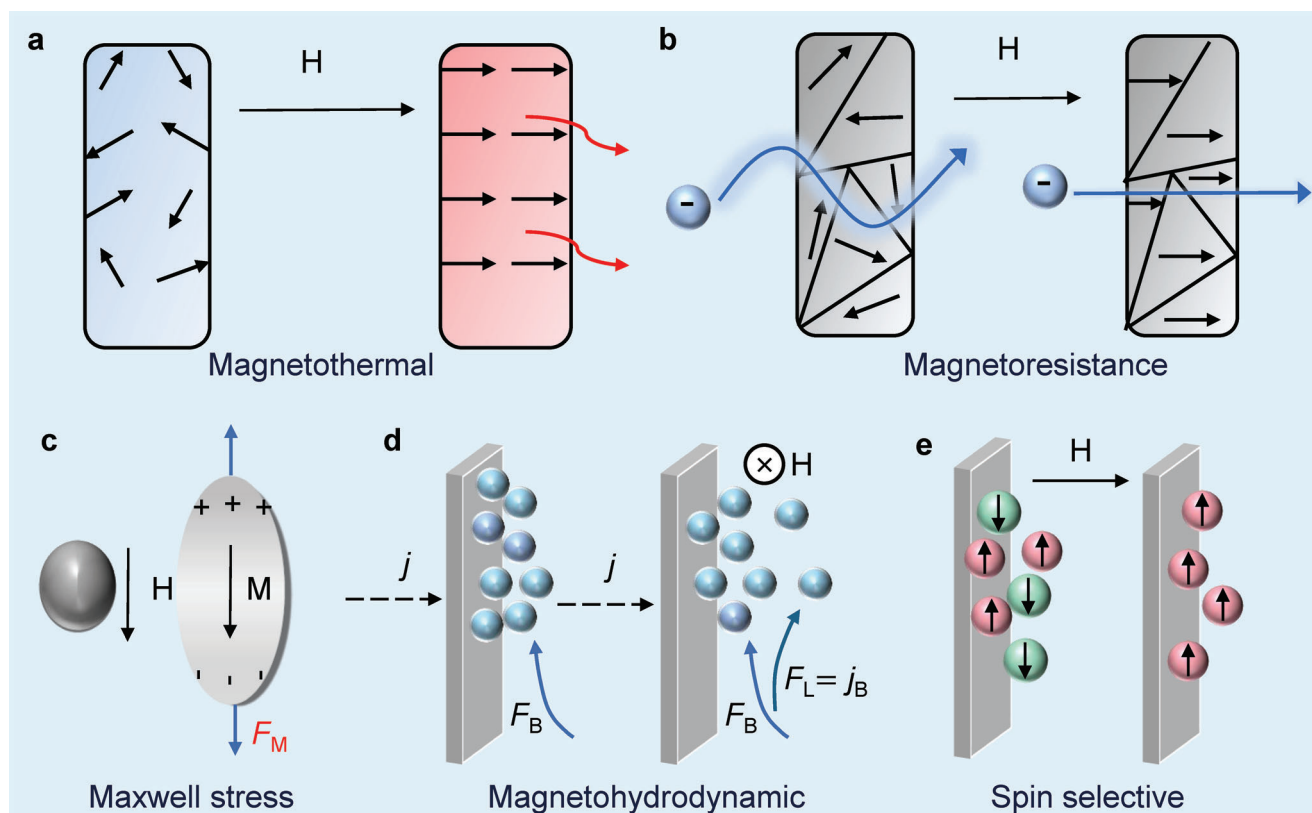


Figure 1. The magnetic effect on the electrocatalytic reaction. a) Magnetothermal effect. b) Magneto-resistance effect. c) Maxwell stress. d) Magneto-hydrodynamic effect. e) Spin selectivity effect.

enhancement is so significant as in alkaline, one can still see the enhanced activities with the increase of AMF.

To understand the influence of magnetic fields on charge transfer behaviors, the electrochemical impedance spectroscopy (EIS) test was conducted (Figure 2d; Figure S4, Supporting Information). Nyquist plots obtained at different magnetic field strengths can be well fitted with the two-semi arcs model. The semi-arc at the low frequency can be attributed to the kinetics of the interfacial charge transfer reaction, while the one at the high frequency corresponds to the dielectric interlayer.^[61] It is surprising to see that the charge transfer resistance is increased with the increase of magnetic field strength, which is contradictory to previous investigations, where increased charge transfer kinetics are generally reported.^[62,63] We proposed that the existence of Lorentz force should be responsible for the increased electron transfer resistance. According to the formula of Lorentz force, the higher the magnetic field intensity, the greater the mass transfer resistance. This makes the mass transfer and the subsequent adsorption at the interface more difficult, thus leading to the observed enhanced electron transfer resistance.

Next, we investigated the influence of geometry by placing the working electrode perpendicularly to the AMF. LSV curves recorded under different AMF strength exhibits similar HER activity enhancement (Figure 2e) as the parallel arrangement. However, the increases are quite different, which are 4.93 and 2.61 mA cm⁻² mT⁻¹ for the parallel and perpendicular geometry, respectively (Figure 2f). The results show that the parallel

arrangement is more effective in boosting the activities. We proposed that the magnetic flux through the working electrodes is different for these two cases. This leads to different induced electromotive forces, which are responsible for the different enhancements. To prove this hypothesis, we investigated the influence of a constant magnetic field produced by a permanent magnet. Indeed, the increase in current density can be ignored because of the absence of induced electromotive force. In addition, we also test the catalytic behavior of Pt wires under the same experimental conditions (Figure S5, Supporting Information). As the magnetic flux through the Pt foil and Pt wires are different, we expect a difference in catalytic efficiency enhancement. At the current density of 330 mA cm⁻² without a magnetic field (Figure S5, Supporting Information), Pt wires require an overpotential of 370 mV. However, the overpotential is decreased to 360 mV with a small AMF of 5 mT, and then rapidly dropped to only 294 mV at 25 mT. When the AMF is 25 mT, the HER current of the Pt foil only increases by 0.5 times. As expected, the enhancement of the HER current of Pt wire is much smaller than that of the Pt foil, whose current is almost doubled with an AMF of 25 mT.

2.3. Induced Electromotive Force in Metal Wires

As we discussed above, the HER measurements under AMF are a complicated system. The AMF could interact with both the metal catalysts and the electrolyte. To uncover the mechanism

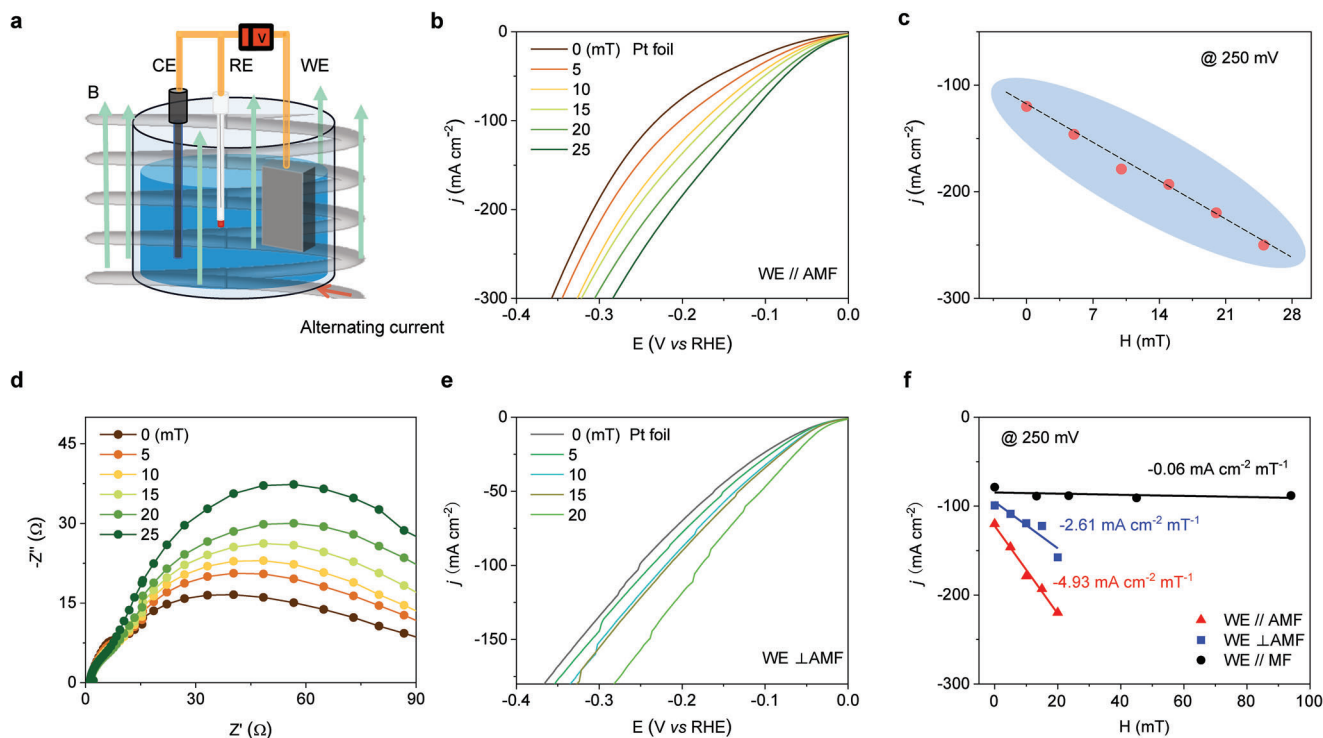


Figure 2. a) Schematic diagram of the HER measurements under vertical AMF (WE and AMF are parallelly arranged, WE||AMF). b) LSV curves for the Pt foil under different AMFs (WE||AMF). c) Comparison of current density at the overpotential of 250 mV. d) The Nyquist plots of the Pt catalyst under different AMFs (WE||AMF). e) LSV curves for the Pt foil under different AMFs (WE⊥AMF). f) The comparison of enhanced HER activities with different relative geometry.

for the magnetic field-enhanced activities, we simplified the catalytic measurements by removing the electrolyte (details can be seen in the experimental section). We thus investigated the response of different metals to the AMF, including paramagnetic Ti and Pt, diamagnetic Cu, and ferromagnetic Ni wires. During the measurements, a constant voltage is applied to the wire, and the current is recorded accordingly with the change of AMF. For Pt wire, there is a rapid decrease in the current once an AMF is applied (Figure 3a). The decrease in the current is proportional to the applied magnetic field and reached zero at 20 mT. The same results were observed when a negative voltage is applied. We then repeat the experiments with ferromagnetic Ni (Figure 3b), paramagnetic Ti (Figure 3c), and diamagnetic Cu wire (Figure 3d). All experiments exhibit similar results except for the critical magnetic fields to reach the zero current.

According to classic Ohm's law, the decreasing and vanishing of the currents can be caused by two possible reasons. The first reason is the significant increase in the resistance of the metal wires in the presence of the AMF. Another one is the real potential of the metal wire is decreased. The first possibility is generally the result of the increased temperature because of the magnetocaloric or eddy current. To exclude the influence of temperature, a 100 Ohm resistor was used and the corresponding temperature is recorded with the infrared thermometer. At a constant voltage, the resistor exhibits the same phenomena as the metal wires (Figure 3e). At the same time, the temperature change of the resistance is monitored during the measurement. It can be seen that when the magnetic field is applied, the temperature of

the resistor increased rapidly from 28.5 °C to ≈33 °C (Figure 3f). The video for such a heating process further confirmed the limited increase in temperature (Video S1, Supporting Information). Considering that the temperature coefficients of most metals are generally below 0.005 TCR/°C, the change in resistivity can be neglected during the experiments. Thus, we conclude that the real potential of the metal wires is changed upon the application of AMF.

2.4. Mechanism for the AMF Enhanced Catalytic Activities

Based on the above experimental results, we believe that the change in catalytic activities and currents is a result of the induced electromotive force produced by the AMF. When the metal catalysts are placed into the AMF, the time-varying magnetic field will create an induced electromotive force, which can be described by the following equation:

$$\oint \vec{E}_{\text{induction}} \cdot d\vec{l} = - \oint \frac{dB}{dt} \cdot dS \quad (1)$$

where l is the effective length of the cutting magnetic field line, B is the variation of magnetic flux, t is time and S is the effective area of the conductor perpendicular to the magnetic flux. The magnitude of the induced electromotive force is proportional to the strength of the magnetic field, the area of the loop, and the rate of change of flux, and is inversely proportional to the resistivity of the material. Most importantly, the geometry of the metal

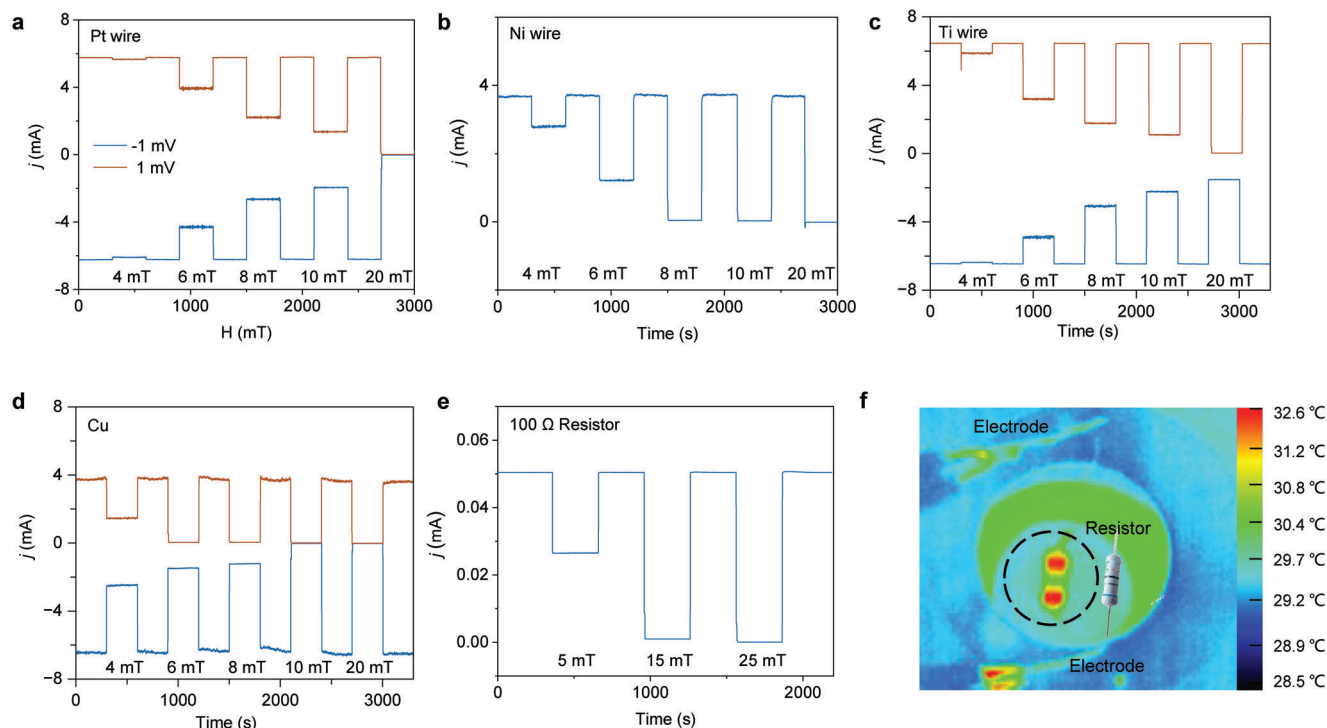


Figure 3. Current changes upon the application of AMF at a constant voltage of 0.0005 V for paramagnetic Pt a) ferromagnetic Ni b), paramagnetic Ti c), and diamagnetic Cu d,e) Current changes of the resistor under different AMFs. f) The temperature profile of the resistor in the presence of an AMF.

electrode and the AMF (Figure 4a), the value for the induced electromotive force may be different.

By considering the frequency of the AMF (104 kHz), the induced electromotive force is calculated to be 0 to 0.26 V when the magnetic field is increased from 0 to 25 mT. This means that in addition to the applied potential from the electrochemical workstation, there is an additive potential that drives the catalytic reactions. Interestingly, the calculated induced electromotive force is in good agreement with the increased HER activities for the Pt foil (Figure 2b).

The above theory can also explain the observed increased charge transfer resistance and solvent resistance. It has been well-studied that the initial step for hydrogen evolution is the

reduction of H^+ or H_2O , depending on the pH value of the electrolyte. The presence of AMF would influence the transport of both electrons and ions in the catalysis process through the Lorentz force. According to the formula of the Lorentz force, $F_L = q \cdot v \times B$, the greater the magnetic field strength, the larger resistance for the mass transfer. This also explains why the mass transfer resistance of the Pt film increases as the overpotential decreases.

3. Conclusion

In summary, we found that the Pt foil has enhanced HER activities in the applied magnetic field. Although the phenomena have

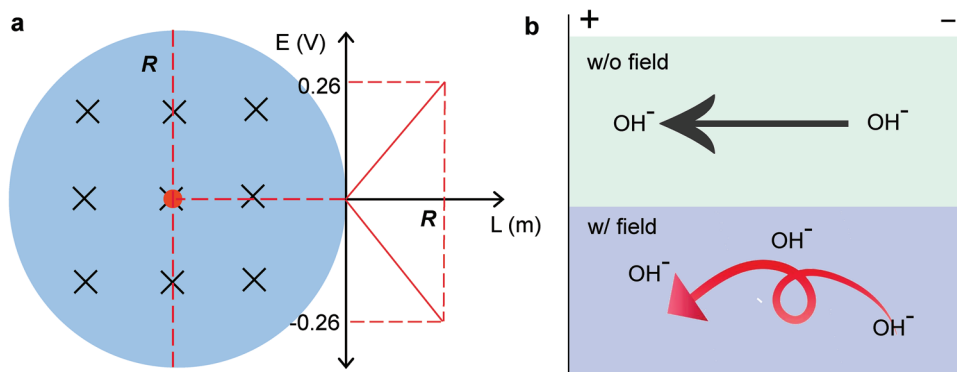


Figure 4. a) The induced electromotive force as a function of the AMF. Maximum potential of 0.26 V is produced under a field of 25 mT. b) The schematic diagram for the mass transport with and without AMF.

been reported before, we found a new possible explanation for the enhanced activities. According to the experimental results, it was found that when an external magnetic field is applied, an induced electromotive force will be generated regardless of their magnetic structures. The magnitude of the emf is closely related to the relative geometry position between the electrodes and the AMFs, and is also somewhat magnetization-dependent. This will increase the real applied voltage of the investigated catalysts and thus boost the HER activities. We exclude the contribution of resistivity and temperature changes because of magnetoresistance or magnetocaloric effect. This work highlights that electrode geometric position should also be considered when using an external magnetic field to assist electrocatalysis. This also provides a feasible idea for designing high-performance catalytic reactions in the future.

4. Experimental Section

Materials Characterization: All reagents were analytical grade and used directly without any further purification. Pt, Ti, Cu, and Ni wires were purchased from Guantai Metal Materials Co., Ltd. Pt foil electrode was purchased from Shanghai Precision Scientific Instrument Co., Ltd. The magnetic field was applied by using QPX1200SP magnetic hyperthermia effect analyzer.

Electrochemical Measurements: All electrochemical measurements were taken on an Autolab PGSTAT302N electrochemistry workstation with an impedance module at room temperature. A typical three-electrode configuration was employed, with the carbon rod worked as the counter electrode and the Ag/AgCl electrode (3 M KCl) as the reference electrode. Metal wires, Pt foils, and resistors served as working electrodes. Linear sweep voltammetry (LSV) experiments were performed at a 2 mV s^{-1} scan rate either in the 1 M KOH or 0.5 M H_2SO_4 electrolytes without iR-compensation. It calculated the current density by the geometrical surface areas of the electrode. All the potentials reported in this work were converted to a reversible hydrogen electrode according to:

$$E \text{ (versus RHE)} = E \text{ (versus Ag/AgCl)} + (0.207 + 0.059 \text{ pH}) \text{ V} \quad (2)$$

Electrochemical impedance spectroscopy (EIS) was performed in a frequency range of 100 kHz–0.1 Hz with an amplitude of 0.01 mV.

Application of Alternating Magnetic Field: All data for alternating magnetic fields were collected using a NAN201006-DS magnetic hyperthermia analyzer at room temperature. The frequency, it chose was 104.0 kHz, the capacitor was 200 nF. The winding method was 17 turns. When performing linear sweep voltammetry (LSV) and electrochemical impedance spectroscopy (EIS) tests, it set the alternating magnetic field application time to 10 min, then waited 30 sec for data collection. When using chronopotential (CP) and chronoamperometry (CA) for testing, it set the magnetic field application time to 180 sec, and the interval between two adjacent magnetic field applications was 180 sec.

Supporting Information

Supporting Information is available from the Wiley Online Library or from the author.

Acknowledgements

S.L. and Y.Z. contributed equally to this work. This work was financially supported by the National Natural Science Foundation of China (52271194), Ningbo Yongjiang Talent Introduction Programme (2022A-090-G), and the Hundred Talents Programs in the Chinese Academy of Science. G. Li

thanks the support from the Max Planck Partner Group program and the Foundation of the director of Ningbo Institute of Materials Technology and Engineering of the Chinese Academy of Sciences.

Conflict of Interest

The authors declare no conflict of interest

Data Availability Statement

The data that support the findings of this study are available from the corresponding author upon reasonable request.

Keywords

hydrogen evolution reaction, induced electromotive force, magnetic fields, magneto-catalysis

Received: June 11, 2023
Revised: August 6, 2023
Published online: August 31, 2023

- [1] F. T. Tsai, Y. T. Deng, C. W. Pao, J. L. Chen, J. F. Lee, K. T. Lai, W. F. Liaw, *J. Mater. Chem. A* **2020**, *8*, 9939.
- [2] C. T. Moi, S. Bhowmick, M. Qureshi, *ACS Appl. Mater. Interfaces* **2021**, *13*, 51151.
- [3] Z. J. Xu, *Nano-Micro Lett.* **2017**, *10* 8.
- [4] N. Zion, L. Peles-Strahl, A. Friedman, D. A. Cullen, L. Elbaz, *ACS Appl. Energ. Mater.* **2022**, *5* 7997.
- [5] W. Li, C. Wang, X. Lu, *Coord. Chem. Rev.* **2022**, *464*, 214555.
- [6] R. Boppella, J. Tan, W. Yang, J. Moon, *Adv. Funct. Mater.* **2019**, *29* 1807976.
- [7] T. Wu, M. Y. Han, Z. J. Xu, *ACS Nano* **2022**, *16* 8531.
- [8] D. Chinnadurai, N. Manivelan, K. Prabakar, *ChemElectroChem* **2022**, *9* e202200254.
- [9] J. Zhang, J. Lian, Q. Jiang, G. Wang, *Chem. Eng. J.* **2022**, *439*, 135634.
- [10] J. Zhang, J. Li, H. Huang, W. Chen, Y. Cui, Y. Li, W. Mao, X. Zhu, X. Li, *Small* **2022**, *18*, 2204557.
- [11] X. He, Z. Hu, R. Guo, Y. Li, L. Wu, *J. Alloy. Compd.* **2023**, *953*, 170190.
- [12] J. X. Feng, Y. X. Tong, G. R. Li, *Chem* **2018**, *4* 2015.
- [13] J. Li, W. Yin, J. Pan, Y. Zhang, F. Wang, L. Wang, Q. Zhao, *Nano Res.* **2023**, *16*, 8638.
- [14] J. Joy, T. Stuyver, S. Shaik, *J. Am. Chem. Soc.* **2020**, *142*, 3836.
- [15] M. Akamatsu, N. Sakai, S. Matile, *J. Am. Chem. Soc.* **2017**, *139*, 6558.
- [16] J. Wang, M. Yan, K. Zhao, X. Liao, P. Wang, X. Pan, W. Yang, L. Mai, *Adv. Mater.* **2017**, *29*, 1604464.
- [17] X. Li, Y. Chen, X. Zhan, Y. Xu, L. Hao, L. Xu, X. Li, M. Umer, X. Tan, B. Han, A. W. Robertson, Z. Sun, *Innovation Mater.* **2023**, *1*, 100014.
- [18] J. Xu, P. Gu, D. J. S. Birch, Y. Chen, *Adv. Funct. Mater.* **2018**, *28*, 1801573.
- [19] X. Cheng, L. Wang, L. Xie, C. Sun, W. Zhao, X. Liu, Z. Zhuang, S. Liu, Q. Zhao, *Chem. Eng. J.* **2022**, *439*, 135757.
- [20] R. Rajendran, K. Varadharajan, V. Jayaraman, B. Singaram, J. Jeyaram, *Appl. Nanosci.* **2018**, *8*, 61.
- [21] M. S. Kodaimati, R. Gao, S. E. Root, G. M. Whitesides, *Chem. Catal.* **2022**, *2*, 797.
- [22] C. Niether, S. Faure, A. Bordet, J. Deseure, M. Chatenet, J. Carrey, B. Chaudret, A. Rouet, *Nat. Energy* **2018**, *3*, 476.
- [23] X. Jiang, Y. Chen, X. Zhang, F. You, J. Yao, H. Yang, B. Y. Xia, *ChemSusChem* **2022**, *15*, e202201551.

- [24] Z. Jiang, S. Song, X. Zheng, X. Liang, Z. Li, H. Gu, Z. Li, Y. Wang, S. Liu, W. Chen, D. Wang, Y. Li, *J. Am. Chem. Soc.* **2022**, *144*, 19619.
- [25] S. Li, J. Liu, Z. Yin, P. Ren, L. Lin, Y. Gong, C. Yang, X. Zheng, R. Cao, S. Yao, Y. D., X. Liu, L. Gu, W. Zhou, J. Zhu, X. Wen, B. Xu, D. Ma, *ACS Catal.* **2020**, *10*, 907.
- [26] X. Liu, S. Gao, Z. Wang, Y. Sun, G. Feng, X. Chen, R. Sa, Q. Li, Z. Ma, *Appl. Surf. Sci.* **2023**, *619*, 156790.
- [27] K. Xu, H. Ding, M. Zhang, M. Chen, Z. Hao, L. Zhang, C. Wu, Y. Xie, *Adv. Mater.* **2017**, *29*, 1606980.
- [28] K. Yoonyoung, W. Motonori, M. Junko, S. Aleksandar, K. Hajime, T. Atsushi, A. Taner, I. Tatsumi, *J. Mater. Chem. A* **2020**, *8*, 1335.
- [29] J. Yao, W. Huang, W. Fang, M. Kuang, N. Jia, H. Ren, D. Liu, C. Lv, C. Liu, J. Xu, Q. Yan, *Small Methods* **2020**, *4*, 2000494.
- [30] C. Wei, Z. J. Xu, *Chinese J. Catal.* **2022**, *43*, 148.
- [31] X. Xu, X. Liu, W. Zhong, G. Liu, L. Zhang, Y. Du, *Ceram. Int.* **2023**, *49*, 16836.
- [32] W. Kiciński, J. P. Sęk, A. Kowalczyk, S. Turczyniak-Surdacka, A. M. Nowicka, S. Dyjak, B. Budner, M. Donten, *J. Energ. Chem.* **2022**, *64*, 296.
- [33] X. G. Gong, Z. Z. Jiang, W. Zeng, C. Hu, X. F. Luo, W. Lei, C. L. Yuan, *Nano. Lett.* **2022**, *22*, 9411.
- [34] T. Sun, Z. Tang, W. Zang, Z. Li, J. Li, Z. Li, L. Cao, J. S. Dominic Rodriguez, C. O. M. Mariano, H. Xu, P. Lyu, X. Hai, H. Lin, X. Sheng, J. Shi, Y. Zheng, Y. R. Lu, Q. He, J. Chen, K. S. Novoselov, C. H. Chuang, S. Xi, X. Luo, J. Lu, *Nat. Nanotechnol.* **2023**, *18*, 763.
- [35] J. Zhang, X. Chen, T. Gao, Y. Wu, Y. Yang, Y. Guo, D. Xiao, *ChemPlusChem* **2021**, *86*, 184.
- [36] Y. Sun, S. Sun, H. Yang, S. Xi, J. Gracia, Z. J. Xu, *Adv. Mater.* **2020**, *32*, 2003297.
- [37] M. Y. Lin, L. W. Hourng, C. W. Kuo, *Int. J. Hydrog. Energy.* **2012**, *37*, 1311.
- [38] C. Biz, M. Fianchini, J. Gracia, *ACS Catal.* **2021**, *11*, 14249.
- [39] C. Biz, M. Fianchini, J. Gracia, *ACS Appl. Nano Mater.* **2020**, *3*, 506.
- [40] C. Biz, M. Fianchini, V. Polo, J. Gracia, *ACS Appl. Mater. Interfaces.* **2020**, *12*, 50484.
- [41] F. A. Garcés-Pineda, M. lasco-Ahícart, D. Nieto-Castro, N. López, J. R. Galán-Mascarós. *Nature Energy.* **2019**, *4*, 519.
- [42] J. Gracia, M. Fianchini, C. Biz, V. Polo, R. Gómez, *Curr. Opin. Electrochem.* **2021**, *30*, 100798.
- [43] T. Wu, X. Ren, Y. Sun, S. Sun, G. Xian, G. G. Scherer, A. C. Fisher, D. Mandler, J. W. Ager, A. Grimaud, J. Wang, C. Shen, H. Yang, J. Gracia, H. J. Gao, Z. J. Xu, *Nat. Commun.* **2021**, *12*, 3634.
- [44] Q. Yang, G. Li, Y. Zhang, J. Liu, J. Rao, T. Heine, C. Felser, Y. Sun, *npj Comput. Mater.* **2021**, *7*, 207.
- [45] Z. W. Fan, P. Zou, K. M. Jiang, W. Xu, M. Gao, V. Zadorozhnyy, G. W. Li, J. T. Huo, J. Q. Wang, *Intermetallics* **2023**, *160*, 107946.
- [46] G. Li, Q. Yang, K. Manna, Q. Mu, C. Fu, Y. Sun, C. Felser, *CCS Chem* **2021**, *3*, 2259.
- [47] L. M. A. Monzon, J. M. D. Coey, *Electrochem. Commun.* **2014**, *42*, 38.
- [48] Y. Zhang, C. Liang, J. Wu, H. Liu, B. Zhang, Z. Jiang, S. Li, P. Xu, *ACS Appl. Energ. Mater.* **2020**, *3*, 10303.
- [49] C. Niether, S. Faure, A. Bordet, J. Deseure, M. Chatenet, J. Carrey, B. Chaudret, A. Rouet, *Nat. Energy.* **2018**, *3*, 476.
- [50] W. Zeng, Z. Jiang, X. Gong, C. Hu, X. Luo, W. Lei, C. Yuan, *Small* **2023**, *19*, 2206155.
- [51] J. Huang, W. Zhou, X. Luo, Y. Ding, D. Peng, M. Chen, H. Zhou, C. Hu, C. Yuan, S. Wang, *Chem. Eng. J.* **2023**, *454*, 140279.
- [52] U. Gupta, C. R. Rajamathi, N. Kumar, G. Li, Y. Sun, C. Shekhar, C. Felser, C. N. R. Rao, *Dalton T* **2020**, *49*, 3398.
- [53] X. Luo, C. Fang, C. Wan, J. Cai, Y. Liu, X. Han, Z. Lu, W. Shi, R. Xiong, Z. Zeng, *Nanotechnology* **2017**, *28*, 145704.
- [54] H. Wang, K. Wang, Y. Zuo, M. Wei, P. Pei, P. Zhang, Z. Chen, N. Shang, *Adv. Funct. Mater.* **2023**, *33*, 2210127.
- [55] J. M. D. Coey, R. Aogaki, F. Byrne, P. Stamenov, *Proc. Natl. Acad. Sci* **2009**, *106*, 8811.
- [56] J. Deng, H. Qiao, C. Li, Z. Huang, S. Luo, X. Qi, *Appl. Surf. Sci.* **2023**, *637*, 157899.
- [57] H. Pan, X. Jiang, X. Wang, Q. Wang, M. Wang, Y. Shen, *J. Phys. Chem. Lett.* **2020**, *11*, 48.
- [58] U. E. Steiner, T. Ulrich, *Chem. Rev.* **1989**, *89*, 51.
- [59] H. Luo, P. Yu, G. Li, K. Yan, *Nat. Rev. Phys.* **2022**, *4* 611.
- [60] Q. Yang, Y. D. Zhang, Y. Sun, C. Felser, G. W. Li, *The Innovation Mater* **2023**, *1*, 100013.
- [61] M. E. Joy, A. K. Tripathi, D. Priyadarshani, D. Choudhury, M. Neergat, *Phys. Chem. Chem. Phys.* **2022**, *24*, 3886.
- [62] L. Cai, J. Huo, P. Zou, G. Li, J. Liu, W. Xu, M. Gao, S. Zhang, J. Wang, *ACS Appl. Mater. Interfaces.* **2022**, *14*, 15243.
- [63] Y. Zhang, P. Guo, S. Li, J. Sun, W. Wang, B. Song, X. Yang, X. Wang, Z. Jiang, G. Wu, P. Xu, *J. Mater. Chem. A* **2022**, *10*, 1760.